

EXPERIMENTAL STUDY ON ENHANCING WELLBORE STABILITY OF COAL MEASURES FORMATION WITH SURFACTANT DRILLING FLUID

Yuliang Zou, Xuming Zhu*, and Xiaoming Wu

The phenomenon of self-cleavage of coal and rocks leads to poor continuity and a high degree of heterogeneity of the coal-rock matrix, causing the wellbore in the process of drilling. The problem of wellbore stability in the drilling process of the coal strata has become one of the key scientific problems. To solve the problem, single-agent optimization and compounding tests of surfactants have been carried out. Based on the test results, the surfactant compounding composition has been selected, which can effectively reduce the surface tension of the drilling fluid and increase the contact angle between the drilling fluid and the coal and rock surface. To evaluate the effect of the drilling fluid wettability on wellbore stability of the coal measures strata, the expansibility test, rolling recovery test, and shale pressure transfer test have been carried out, combined with the basic performance tests of the water-based drilling fluid. The results show that the composite surfactant can effectively reduce the surface tension of the drilling fluid by 80.83% and increase the contact angle with coal by 54.17%. The recovery rate of the composite surfactant water-based drilling fluid is as high as 96.2%. The compound surfactant drilling fluid can significantly slow down the transfer rate of shale pore pressure, reduce the invasion degree of the drilling fluid to coal and rock matrix, prevent hydration erosion, and effectively enhance the stability of coal and rock sidewall.

Keywords: *surface-active agent, coal measures strata, drilling fluid, sidewall stability.*

Faculty of Engineering, China University of Geosciences, Wuhan, 430074, China. *Corresponding author: Xuming Zhu. E-mail: zxm@cug.edu.cn.* Translated from *Khimiya i Tekhnologiya Topliv i Masel*, No. 1, pp. 100 – 104, January – February, 2021.

INTRODUCTION

Coalbed methane is an unconventional natural gas generated and stored in a coal-bearing formation. With substantial global reserves and wide distribution, coalbed methane is one of the essential traditional energy sources in the world [1-3]. Coalbed methane development technology has aroused widespread concern in the industry. In drilling engineering, coal and rock formations are characterized by anisotropic discontinuities, cleavages, voids, and fissures. Due to heterogeneity, sidewall collapse accidents are easy to occur [4-6]. Coal seam sidewall instability will not only lead to drilling difficulties, sticking accident, and reduced drilling efficiency, but also pose a severe threat to engineering safety and quality [7, 8]. The research on the sidewall stability of coal seam in the process of coalbed methane mining has become one of the fundamental scientific problems to be solved urgently [9]. In the process of coalbed methane development, the design of a drilling fluid system is one of the most important key technologies, determining the success or failure of coalbed methane drilling engineering and reservoir protection.

The interaction between the oil and water fluid and the reservoir rocks is defined by wettability, which is usually characterized by the contact angle (θ) of the liquid on the rock surface. Wettability is generally defined as water wetting when $\theta < 75^\circ$, neutral wetting when $\theta > 75^\circ$, and oil wetting when $\theta > 105^\circ$ [10, 11]. When put in contact with ordinary liquids, coal and rock matrix is easily hydrated and destroyed. In the earlier published studies, the researchers reported that an increase in the wetting angle and reduction of the drilling fluid surface tension can reduce the intrusive damage of the coal seam and enhance the stability of coal measures strata [12-14].

A number of scholars have used traditional techniques to enhance the wellbore stability of coal measures strata, including using positive glue to restrain coal seam hydration and pH control of a water-based drilling fluid [15-17]. However, the traditional wellbore stabilization technology and methods do not provide a comprehensive solution to the wellbore stability problem in a coal measures strata. In this paper, we have developed the optimal formula and implementation scheme of water-based drilling fluid for ensuring the wellbore stability in a coal measures strata.

The formula of surfactant drilling fluid which can effectively reduce the surface tension of drilling fluid and increase the contact angle between drilling fluid and coal is optimized, combined with a basic performance test, expansibility test, rolling recovery test, and shale pressure transfer test of the water-based drilling fluid. To enhance the stability of the coal measures formation, the surfactant drilling fluid system is studied, and the rheology, filtration, wettability, inhibition, and other properties of the drilling fluid are comprehensively evaluated.

1 EXPERIMENTAL MATERIALS AND INSTRUMENTS

1.1 EXPERIMENTAL MATERIALS

The coal samples are obtained from the Permian Shanxi formation in Jincheng, Shanxi Province (hereinafter referred to as “Shanxi formation coal”), and the sampling depth is about 660 m. The chemical reagents include: non-ionic surfactant FC-1, anionic surfactant ASA-1, cationic surfactant (Shanxi formation coal surfactant) CS-1, amphoteric surfactant AMS-1, Jianping sodium bentonite, plant gum (LG), anhydrous sodium carbonate (Na_2CO_3), potassium chloride (KCl), calcium sulfate (Ca_2SO_4), iron-chromium lignosulfonate (FCLS), high viscosity carboxymethyl cellulose sodium salt (HV-CMC), and polyacrylamide (PAM).

Based on laboratory experiments, the optimized formula of the water-based drilling fluid is: water + 5% Jianping sodium bentonite + 0.25% Na_2CO_3 + 0.4% Ca_2SO_4 + 1% FCLS + 4% KCl + 1.5% LG + 2% HV-CMC + 0.01% PAM.

1.2 EXPERIMENTAL EQUIPMENT

Scanning electron microscope ZEISS EVO18 tungsten filament series, HKY-3 PertPRODY2198 X-ray diffractometer, HKY-3 shale pressure transfer detector, ZNP-1 dilatometer, ZNN-D6S six-speed rotary viscometer, ZNS-5A medium pressure water loss meter, QBZY automatic surface tensiometer, JC2000DM contact angle meter, EP extreme pressure lubrication instrument, LabSwift water activity meter, JHP core press, LCMP-1A metallographic sample grinding and polishing machine, and XGRL-4 high-temperature roller reheating furnace.

2 EXPERIMENTAL METHOD

2.1 X-RAY DIFFRACTION AND MICROSTRUCTURE ANALYSIS OF ROCK SAMPLES

The X-ray diffraction method is an effective key technique for studying the microstructure of rocks [18-20]. The mineral composition of coal and rock samples is analyzed by the X-ray diffraction test. The test results are shown in Table 1 and Fig. 1.

The coal rocks of Shanxi formation are mainly semi-bright briquette and semi-dark briquette, with a small amount of dull type. The coal samples have grease luster and are easily broken. The coal rocks of Shanxi formation are mainly primary coal, showing apparent heterogeneity and anisotropy. The results of the X-ray diffraction composition analysis show that the coal contains 11% of illite and chlorite minerals, that have a strong water sensitivity. The quartz content accounts for 12% and the amorphous content accounts for 68%. The brittleness index of the samples is high, the clay mineral content is medium, and the hydration expansion effect is more pronounced.

Table 1

Sample	Illite	Chlorite	Dickite	Feldspar	Kaolinite	Quartz	Calcite	Dolomite	Amorphous
Coal and rock of Shanxi formation	7	4	4	0	0	12	5	0	68

Table 2

Compound formula	Contact angle, °	Surface tension, $\text{mN}\cdot\text{m}^{-1}$
Water	31.92	62.31
Water + 0.15% FC-1	46.58	36.81
Water + 0.25% ASA-1	51.66	42.56
Water + 0.35% CS-1	57.25	45.19
Water + 0.45% AMS-1	42.31	39.13
Water based drilling fluid	24.42	53.45
Water based drilling fluid + 0.25% ASA-1 + 0.35% CS-1	53.71	31.87
Water based drilling fluid + 0.15% FC-1 + 0.45% AMS-1	57.69	28.56

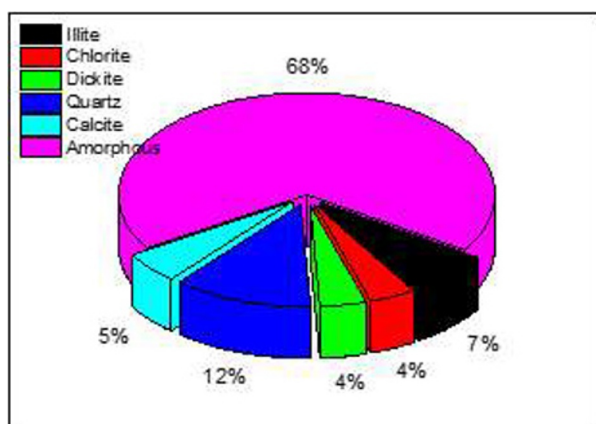


Fig. 1. Mineral composition of coal and rock samples.

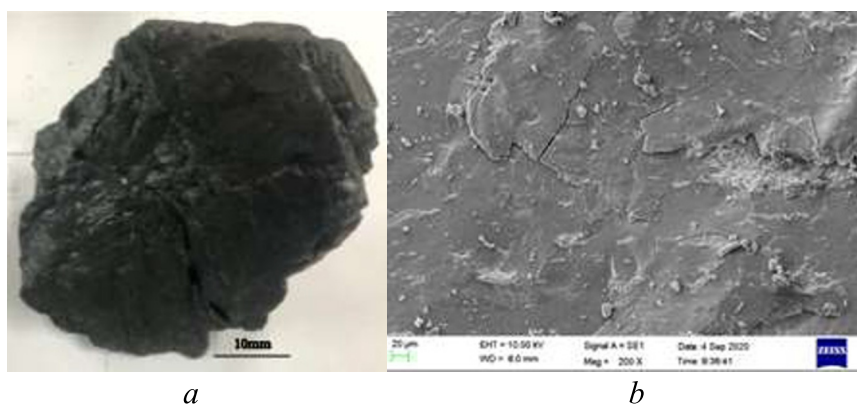


Fig. 2. Physical diagram of coal and rock samples (a) and SEM diagram of coal and rock (b).

The coal and rock samples are shown in Fig. 2a. It can be seen, that the samples are massive in appearance, the surface is relatively smooth, the structure of the silk group is loose, and the surface exhibits obvious fractures and cracks. The microscopic morphology of coal and rock samples of Shanxi formation was observed by the ZEISS EVO18 scanning electron microscope, as shown in Fig. 2b. It can be seen, that the coal structure consists of micro-nano structure pores, fissures, and cleavages. The microfractures are mainly tensional fissures, and the developed shear fissures can be observed. These voids and cleavages constitute fast channels for mud invasion, causing rapid hydration and disintegration of coal and rocks and affecting the wellbore stability of coal measures strata.

2.2 OPTIMIZATION OF COMPOUND SURFACTANT FORMULA

In order to increase the contact angle of the Shanxi formation coal and to reduce the surface tension of the solution, the four types of surfactants were compounded by an orthogonal experiment. The surfactants include non-ionic surfactants, anionic surfactants, cationic surfactants, and amphoteric surfactants. The optimized formula of a compound surfactant drilling fluid system is obtained as follows: the water-based drilling fluid + 0.15% FC-1 + 0.45% AMS-1. The compound fluid can sufficiently increase the contact angle with the coal and rock samples of Shanxi formation, and reduce the surface tension of the solution, as shown in Table 2.

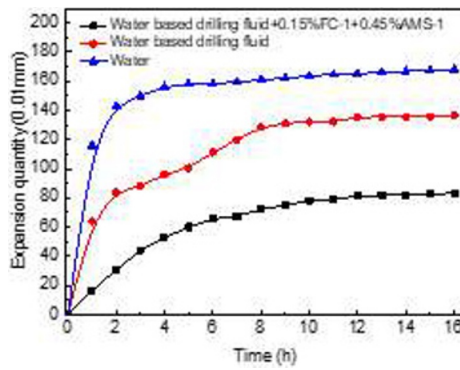


Fig.3. Comparative diagram of coal and rock expansion of Shanxi formation.

2.3 EFFECT OF COMPOUND SURFACTANT ON THE PERFORMANCE OF THE WATER-BASED DRILLING FLUID

2.3.1 Basic performance

For the optimized compound surfactant drilling fluid system (water-based drilling fluid + 0.15% FC-1 + 0.45% AMS-1), the apparent viscosity, plastic viscosity, dynamic shear force, filtrate loss, density, and pH parameters were tested at room temperature. The results are presented in Table 3.

Table 3.

2.3.2 Expansibility

The coal and rock samples were crushed through a 40-mesh sieve, and the amount of 15g of coal powder was weighed and placed in the test chamber. The coal powder was compressed in a core compactor for 60 minutes under the pressure of 8 MPa, the resulting cylindrical core samples have a length of 16 mm and diameter of 25 mm. In the ZNP-1 dilatometer, the artificial cylindrical coal and rock samples are placed in water-based drilling fluid and compound surfactant water-based drilling fluid, respectively, and the real-time expansion parameters of coal and rock samples are recorded. The control time is 16 hours, and the results are shown in Fig. 3.

2.3.3 Rolling recovery rate

The Shanxi coal and rock samples were crushed through a 40-mesh sieve, and the amount of 50g of powder was placed in the aging tanks containing clear water, water-based drilling fluid, and compound surfactant drilling fluid, respectively. The aging tank was heated in an XGRL-4 high-temperature roller heating furnace at 80°C for 16 h; then the sample was washed and dried at 100°C for 6 h. After cooling for eight hours, the coal sample was weighed, and then the rolling recovery rate was calculated. The results are shown in Table 4.

2.4 SHALE PRESSURE TRANSFER TEST

The pressure transfer test is used to evaluate the characteristics and effect of drilling fluid additives on restraining the pressure transfer. Under the same experimental conditions, when the upstream pressure transfer to the downstream is slower, the shale inhibition ability of the drilling fluid is stronger, and the rock strata tend to be stable. To evaluate the effect of compound surfactant on coal and rock sidewall stability, the pressure transfer experiments of different fluids and coal cores were carried out by using the HKY-3 shale pressure transfer experimental device. The experimental conditions are as follows: the confining pressure is 3.5 MPa, the

Table 3

Formula	AV, mPa·s	PV, mPa·s	YP, Pa	FL, ml	P	pH
Water based drilling fluid	18	18.5	6.2	12.4	1.052	8
Water based drilling fluid + 0.15% FC-1 + 0.45% AMS-1	19.2	19.6	5.7	9.7	1.061	8

Table 4

Formula	Pre-test mass / g	Post-test mass / g	Recovery rate / %
Water	50	43.7	87.4
Water based drilling fluid	50	47.6	95.2
Water based drilling fluid + 0.15% FC-1 + 0.45% AMS-1	50	48.1	96.2

Table 5

Formula	Test time / h	Coal permeability , 10^{-18} m^2	Permeability reduction rate / %
Water	7	47.24	—
Water+0.35%CS-1	9	6.88	84.56
Water+0.25%ASA-1	30	4.35	96.89
Water+0.45% AMS-1	33	0.113	97.56
Water+0.15%FC-1+0.45%AMS-1	35	0.109	98.74

upstream pressure is maintained at 2.5 MPa, and the data recording frequency is 1/1 min. The pressure transfer experimental curve and calculated shale permeability results are presented in Fig. 4.

3 EXPERIMENTAL RESULTS AND DISCUSSION

3.1 OPTIMIZATION OF COMPOUND SURFACTANT FORMULA

The results of the surfactant formula optimization are shown in Table 2. The results show that when the water-based drilling fluid contains one type of surfactant, specifically a non-ionic surfactant FC-1, anionic surfactant ASA-1, cationic surfactant CS-1, or amphoteric surfactant AMS-1, it can enhance the Shanxi coal wettability to some extent, but the effect is not very obvious. Through the compounding of 0.15% FC-1 and 0.45% AMS-1, the contact angle with coal and rock surface increases from 31.92° to 57.69° , an increase of 80.83%, and the surface tension of water-based drilling fluid decreases from 62.32 to $28.56 \text{ mN}\cdot\text{m}^{-1}$, a decrease of 54.17%.

It shows that the effect of compound surfactant on improving the wettability of drilling fluid is excellent. The main reason is that the non-polar group of fluorocarbon surfactant is fluorocarbon chain, that is, the hydrogen atoms of the hydrocarbon chain are partially or entirely replaced by a fluorine atom, which leads to the characteristics of high electronegativity, difficulty to be polarized, and large atomic radius of the fluorine group in FC-1. The fluorine-carbon bond energy is high, it is difficult to be destroyed, and the fluorine atom has a shielding effect on the carbon-carbon bond. The fluorocarbon chain has a more substantial hydrophobic effect than the hydrocarbon chain, resulting in a neat and stable hydrophobic layer on the coal surface. At the same time, the amphoteric surfactant AMS-1 mainly gives a synergistic effect.

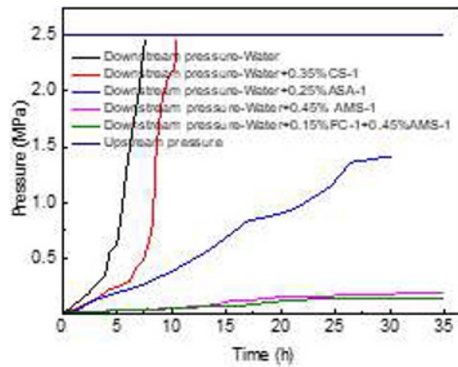


Fig. 4. Pressure transfer test results of rock samples under different solutions.

3.2 EFFECT OF COMPOUND SURFACTANT ON THE PERFORMANCE OF WATER-BASED DRILLING FLUID

The effect of composite surfactant on the fundamental properties of water-based drilling fluid is shown in Table 3. It can be seen that after adding 0.15% FC-1 + 0.45% AMS-1 composite surfactant, the apparent viscosity, plastic viscosity, dynamic shear force, filtrate loss, density, and pH of water-based drilling fluid do not change significantly. The changes in viscosity and test water volume are moderate, indicating that the composite surfactant has good compatibility with water-based drilling fluid. As can be seen from Fig.3 and Table 4, the expansion of coal and rock is only 1.63 mm after soaking in water-based drilling fluid for 16 h, while the expansion of coal and rock in compound surfactant water-based drilling fluid is only 0.72 mm, indicating that in the compound surfactant the expansion of coal and rock samples decrease by 55.83%.

In the rolling recovery test, the results show the presence of micro-nano pores and cracks in the coal structure, and there are different degrees of debris filling in the cracks. The hydration characteristics are apparent and the recovery rate in water is only 87.4%. However, the recovery rate in composite surfactant water-based drilling fluid is 96.2%, indicating that composite surfactant can improve the inhibition ability of water-based drilling fluid, reduce the water lock effect, and reduce the water contact between coal and water-based drilling fluid, thus inhibiting the hydration expansion of shale.

3.3 COAL-ROCK PRESSURE TRANSFER EXPERIMENT

As can be seen from Figs. 4 and 5, when using clear water, the upstream pressure is completely transferred to the downstream within 7 h, and the calculated shale permeability is $4.72 \times 10^{-17} \text{ m}^2$. Using a single surfactant formula - water + 0.45% AMS-1, the upstream pressure is completely transferred to the downstream within 33 h, and the calculated shale permeability is $1.13 \times 10^{-19} \text{ m}^2$. Using a compound surfactant formula - water + 0.15% FC-1 + 0.45% AMS-1, the upstream pressure is completely transferred to the downstream within 35 h, and the calculated shale permeability is reduced to $1.09 \times 10^{-19} \text{ m}^2$.

The results show that compared with a single surfactant, the optimized composite surfactant formula is more effective in retarding pressure transfer and enhancing coal-rock sidewall stability. Due to the synergism between composite surfactants, the effect can enhance the hydrophobicity of coal and drilling fluid, hinder pore pressure transfer, reduce the invasion degree of drilling fluid to coal and rock, and achieve the purpose of enhancing shale wellbore stability.

4 CONCLUSIONS

(1) Through the hydrophobic action of fluorocarbon surfactant and the synergistic effect of amphoteric surfactant, the compound surfactants (0.15% FC-1 and 0.45% AMS-1) can effectively reduce the surface tension

of coal-rock water-based drilling fluid, increase the contact angle between drilling fluid and coal-rock, and change the wettability of water-based drilling fluid.

(2) The apparent viscosity, plastic viscosity, dynamic shear force, filtrate loss, density, and pH parameters of the composite surfactant water-based drilling fluid change insignificantly, and the viscosity and test water volume are moderate, indicating that the composite surfactant and water-based drilling fluid have good compatibility, can increase the inhibition of water-based drilling fluid, and can more effectively restrain the hydration and expansion of shale.

(3) The synergism between surfactants can enhance the hydrophobicity of coal and drilling fluid, hinder the transfer of pore pressure, reduce shale permeability, reduce the invasion of drilling fluid into coal and rock, and prevent hydration and erosion of coal and rock. Therefore, it can effectively enhance the stability of coal and rock sidewall.

REFERENCE

1. K. G. J. Chand and R. Chatterjee, "Impact of geomechanics in coal bed methane development and production, Barakar coals in Central India," *J. Pet. Sci. Eng.*, 194, 107515 (2020).
2. S. Emmert, H. Class, K. J. Davis, et al., "Importance of specific substrate utilization by microbes in microbially enhanced coal-bed methane production: a modelling study," *Int. J. Coal Geol.*, 229, 103567 (2020).
3. R. Rathi, M. Lavania, N. Singh, et al., "Evaluating indigenous diversity and its potential for microbial methane generation from thermogenic coal bed methane reservoir," *Fuel*, 250, 362-372 (2019).
4. H. L. Ramandi, M. A. Pirzada, S. Saydam, et al., "Digital and experimental rock analysis of proppant injection into naturally fractured coal," *Fuel*, 286, 119368 (2021).
5. M. Wiêckowski and N. Howaniec, "Natural desorption of carbon monoxide during the crushing," *Sci. Total Environ.*, 736, 139639 (2020).
6. M. Brook, B. Hebblewhite and R. Mitra, "Coal mine roof rating (CMRR), rock mass rating (RMR) and strata control: Carborough Downs mine, Bowen Basin, Australia," *Int. J. Min. Sci. Technol.*, 30(2), 225-234 (2020).
7. M. Mukherjee and S. Misra, "A review of experimental research on enhanced coal bed methane (ECBM) recovery via CO₂ sequestration," *Earth Sci. Rev.*, 179, 392-410 (2018).
8. A. Y. Oudinot and D. E. Riestenberg, "Enhanced gas recovery and CO₂ storage in coal bed methane reservoirs with N₂ co-injection," *Energy Proc.*, 114, 5356-5376 (2017).
9. K. Iyer and D. W. Schmid, "Comment on "Thickness matters: influence of Dolerite Sills on the thermal maturity of surrounding rocks in a coal bed methane play in Botswana" by Bulguroglu and Milkov (2020)," *Mar. Pet. Geol.*, 115, 104247 (2020).
10. S. Zhang and H. Pei, "Rate of capillary rise in quartz nanochannels considering the dynamic contact angle by using molecular dynamics," *Powder Technol.*, 372, 477-485 (2020).
11. E. Sadeghinezhad, M. A. Q. Siddiqui, et al., "On the interpretation of contact angle for geomaterial wettability: contact area versus three-phase contact line," *J. Pet. Sci. Eng.*, 195, 107579 (2020).
12. Z. Guo, L. Wang, R. Hakkou, et al., "Determination of the contact angles and pseudo-line tensions on heterogeneous surfaces with different size of bubbles," *Colloid. Surf. A: Physicochem. Eng. Asp.*, 611, 125772 (2020).
13. D. Blanco, N. Rivera, et al., "Novel fatty acid anion-based ionic liquids: contact angle, surface tension, polarity fraction, and spreading parameter," *J. Mol. Liq.*, 288, 110995 (2019).

14. C. Chao and G. Xu, "Effect of surface tension, viscosity, pore geometry and pore contact angle on effective pore throat," *Chem. Eng. Sci.*, 197, 269-279 (2019).
15. J. Zuo, Y. Lin, P. Zhong, et al., "Investigation on adhesive wear process of tool coating surface under high-adhesive rate environment in cutting beryllium-copper C17200 alloy," *Mater. Lett.*, 279, 128488 (2020).
16. M. A. Isa and O. B. Bodnar, "Hyaluronic acid solution as a treatment of adhesive intestinal obstruction in children – a positive effect," *Porto Biomed. J.*, 2(5), 246 (2017).
17. A. De Ponti, M. G. Viganò, et al., "Adhesive capsulitis of the shoulder in human immunodeficiency" *J. Should. Surg.*, 15(2), 188-190 (2006).
18. C. Iatosti, M. Moret, et al., "Analysis of the gallium gradient in $\text{Cu}(\text{In}_{1-x}\text{Ga}_x)\text{Se}_2$ absorbers by X-ray diffraction," *Sol. Energ. Mater. Sol. Cells*, 220, 110847 (2021).
19. N. Viganò and W. Ludwig, "X-Ray orientation microscopy using topo-tomography and multi-mode diffraction contrast tomography," *Curr. Opin. Solid State Mater. Sci.*, 24(4), 100832 (2020).
20. G. S. Harlow and E. Lundgren, "Recent advances in surface X-Ray diffraction and the potential for determining structure-sensitivity relations in single-crystal electrocatalysis," *Curr. Opin. Electrochem.*, 23, 162-173 (2020).
21. G. Lillo, R. Mastrullo, A. W. Mauro, et al., "Flow boiling heat transfer: experiments and assessment of predictive methods," *Int. J. Heat Mass. Tran.*, 126, 1236-1252 (2018).
22. V. Solotych, D. Lee, J. Kim, et al., "Boiling heat transfer and two-phase pressure drops within compact plate heat exchangers: experiments and flow visualizations," *Int. J. Heat Mass. Tran.*, 94, 239-253 (2016).
23. A. Diani, K. K. Bodla, et al., "Numerical investigation of pressure drop and heat transfer through reconstructed metal foams and comparison against experiments," *Int. J. Heat Mass. Tran.*, 88, 508-515 (2015).
24. S. Grauso, R. Mastrullo, A. W. Mauro, et al., "Flow pattern map," *Int. J. Refrig.*, 36(2), 478-491 (2013).
25. A. Koyuncuođlu, R. Jafari, T. Okutucu-Özyurt, et al., "Heat transfer and pressure drop experiments on CMOS compatible microchannel heat sinks for monolithic chip cooling applications," *Int. J. Therm. Sci.*, 56, 77-85 (2012).